

RADIO FREQUENCY SYSTEMS

M. A. Honnell, Project Leader

MILLIMETER WAVES STUDY

E. R. Graf, Project Leader

PREPARED BY

MICROWAVE RESEARCH LABORATORY

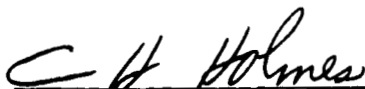
TENTH QUARTERLY REPORT

1 June 1966 to 1 September 1966

CONTRACT NAS8-11184


GEORGE C. MARSHALL SPACE FLIGHT CENTER  
NATIONAL AERONAUTICS AND SPACE ADMINISTRATION  
HUNTSVILLE, ALABAMA

APPROVED BY:



C. H. Holmes  
Head Professor  
Electrical Engineering

SUBMITTED BY:



M. A. Honnell  
Professor of Electrical Engineering  
and Project Leader

## FOREWORD

This report summarizes the progress of the Auburn University Electrical Engineering Department toward fulfillment of the requirements in NASA Contract NAS8-11184. The contract is administered by the Auburn Research Foundation.

Monthly progress letters have been submitted prior to this report. Contract progress has been reviewed by telephone and also in meetings with Mr. T. A. Barr, Contract Supervisor, National Aeronautics and Space Administration, Huntsville, Alabama.

## TABLE OF CONTENTS

FOREWORD.....	ii
LIST OF FIGURES.....	iii
INTRODUCTION.....	1
I. RADIO FREQUENCY SYSTEMS.....	2
A. 2280-MHz Television Exciter Unit	
B. Description of the Planned 1720-MHz FM Transmitter	
1. Exciter Unit	
a. Video Amplifier and Clamping Circuit	
b. Voltage-Controlled Oscillator	
c. Transistor Frequency Multiplier	
d. Radio-Frequency Amplifier Chain	
e. Diode Frequency Multiplier	
f. Automatic Frequency Control Loop	
g. Keying Pulse Generator	
h. Dc to Dc Converter	
2. Power Amplifier Unit	
C. Exciter AFC Systems Analyses	
D. Peltier Temperature Chamber	
II. MILLIMETER WAVES STUDY.....	39

## LIST OF FIGURES

1. A Block Diagram of the Proposed 1720-MHz FM Transmitter.
2. End View of the Proposed Transmitter Cases.
3. Side View of the Proposed Transmitter Cases.
4. A Block Diagram of Proposed 1720 MHz exciter.
5. A Block Diagram of the Proposed Dc to Dc Converter for the Exciter.
6. Block Diagram of an Intermediate-Frequency Discriminator AFC System.
7. Simplified Block Diagram of an Intermediate-Frequency Discriminator AFC System.
8. Further Simplified Block Diagram of an Intermediate-Frequency Discriminator AFC System.
9. Curves Showing the Output Frequency Stability Factor as a Function of Open-loop Gain  $K$ , VCO Stability Factor  $\delta_V$ , and Discriminator Stability Factor  $\delta_D$ . The Reference Oscillator Stability Factor  $\delta_R$  Is Assumed to Be .002 Percent and  $f'_D/f'_0 = 0.1$ .
10. Curves Showing the Required Open-loop Gain  $K$  for a Required Output Stability Factor of .005 Percent as a Function of the Discriminator Stability Factor  $\delta_D$  and the VCO Stability Factor  $\delta_V$ . The Reference Oscillator Stability Factor  $\delta_R$  Is Assumed to Be .002 Percent and  $f'_D/f'_0 = 0.1$ .
11. Block Diagrams of the Parallel Discriminator (a) and the Composite Discriminator (b).
12. Idealized Discriminator Curves for a Wide-Band (a) and a Narrow-Band (b) Discriminator and a Composite Curve (c) for the Two in Parallel. The Composite Curve Has Three Zero-Crossings Due to a Center Frequency Drift of the Wide-Band Discriminator That is Greater Than One-Half the Bandwidth of the Narrow-Band Discriminator.
13. Block Diagram of a Gated Discriminator AFC System Operating at the VCO Frequency.
14. Simplified Block Diagram of a Gated Discriminator AFC System Operating at the VCO Frequency.

15. Curves of the Output Stability Factor  $\delta_o$  as a Function of the Open-loop Gain  $K$ , the VCO Stability Factor  $\delta_v$ , and the Ratio  $K_R/K_o$ . The Reference Stability Factor  $\delta_R$  and Discriminator Stability Factor  $\delta_D$  Are Assumed Constant at  $\pm 0.002$  Percent and  $\pm 0.5$  Percent Respectively.
16. A Block Diagram of the Peltier Thermoelectric Environmental Chamber.

## INTRODUCTION

The final two models of the 2280-MHz FM television exciter unit were completed and delivered to the NASA Astrionics Laboratory at Huntsville, Alabama.

The required design specifications for the 1720-MHz FM transmitter, and a complete description of the proposed transmitter operation, are presented in this report. An analysis of two types of automatic frequency control systems, which can provide the required frequency stability, is also given in this report.

An analytical and experimental study of the effects of bandwidth-limited, frequency-modulated, transmitter systems was made. Also, the effect of synchronous clamping in such a bandwidth-limited system was investigated. The results of these tests were presented in a special technical report dated July 15, 1966.

A review of progress made on the Millimeter Waves Study is included in the last section of this report.

## I. RADIO FREQUENCY SYSTEMS

M. A. Honnell, W. E. Faust, H. L. Deffebach, and W. W. Agerton

### A. 2280-MHz Television Exciter Unit

Serial numbers 7 and 8 of the Model S-1 series of the 2280-MHz FM television exciter unit were completed and delivered to the NASA Astrionics Laboratory at Huntsville, Alabama.

### B. Description of the Planned 1720-MHz FM Transmitter

A 1720-MHz FM transmitter that will transmit high-quality video information from a space vehicle to a ground receiving station is planned. The required design specifications for the transmitter are as follows:

1. A video input impedance of 75 ohms.
2. A video input signal of 1.4 volts peak-to-peak.
3. Video circuits to accommodate either polarity of input signal.
4. A video bandwidth of 5 Hz to 10 MHz ( $\pm 1$  db).
5. A provision for a pre-emphasis network.
6. An RF bandwidth of 20 MHz (flat to  $\pm 1.0$  db) from 1710 MHz to 1730 MHz.
7. A frequency-modulated radio-frequency output of 20 watts into 50 ohms.
8. A frequency stability requirement of .01 percent for the temperature range of  $-20^{\circ}\text{C}$  to  $80^{\circ}\text{C}$ .
9. A capability of being switched on or off from a remote location.

10. A capability to transmit high-quality video information while subjected to random vibrations of 20 to 2000 Hz at 21 G's for four seconds along each of the three major axes, and 20 to 2000 Hz at 16 G's for 3 minutes along each of the three major axes.
11. A case capable of being pressurized.

The proposed transmitter is shown in block diagram form in Figure 1. As indicated, the transmitter has two distinct sections: (1) the exciter unit, comprising the exciter and an accompanying dc to dc converter, and (2) the power amplifier unit, employing two cavity-type amplifiers and an accompanying dc to dc converter. The exciter unit will accept a video input of 1.4 volts peak-to-peak, and will provide a frequency-modulated radio-frequency output of 0.5 watts. The power amplifier will amplify the radio-frequency output of the exciter unit to 20 watts.

The transmitter's physical configuration will consist of two separate units, one mounted atop the other. The exciter and its associated power supply will be contained in the first unit and the power amplifiers and their power supply in the second unit. Drawings of the proposed cases and their mounting are shown in Figures 2 and 3.

Each unit will be complete and requires no accessories to perform its intended function. Each will be capable of being pressurized and will meet environmental and other flight requirements. Because of these characteristics, each can be used separately for other application.

Internally, the exciter case will be designed to allow mounting of modular-type circuit boards. The layout will be such that it allows access to



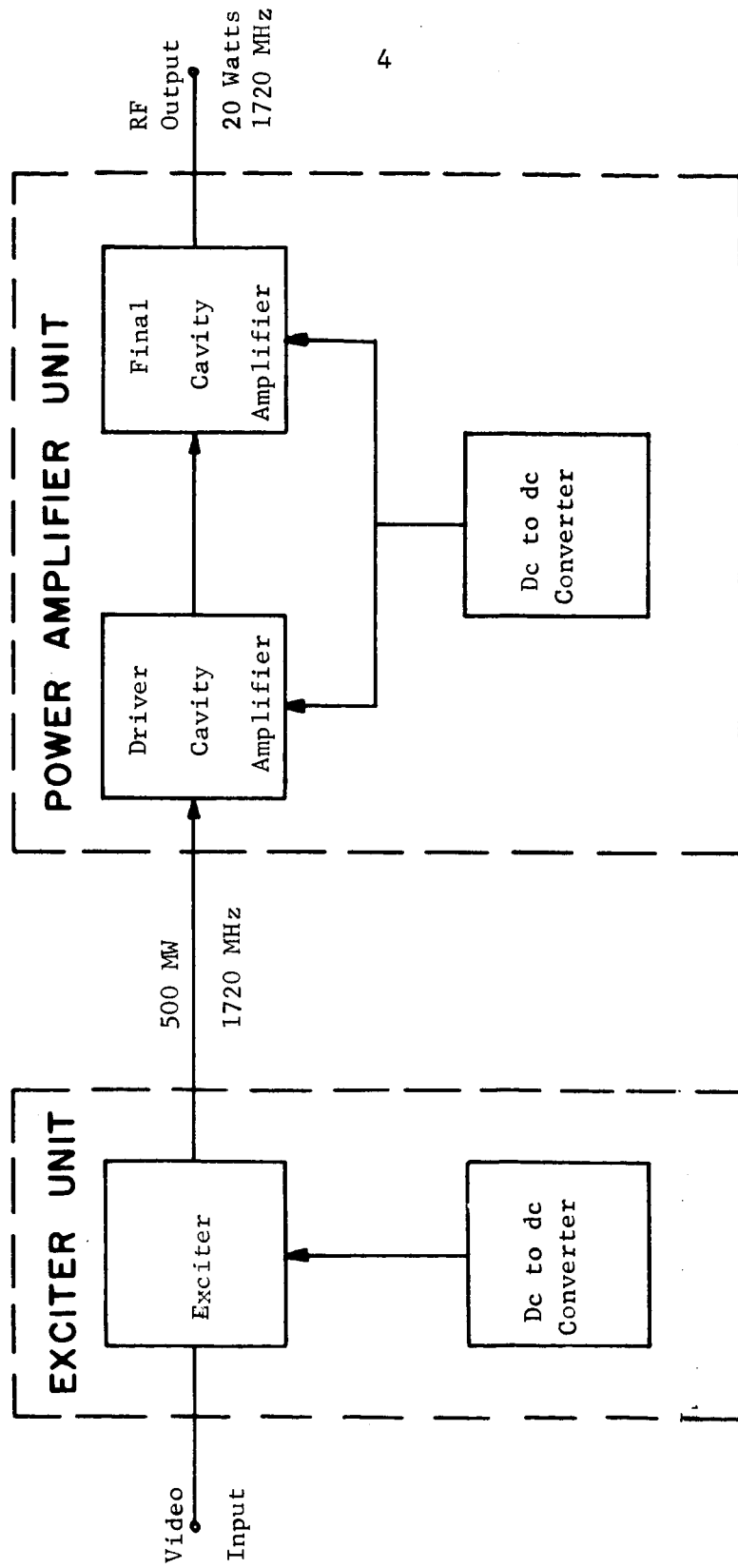


Fig. 1--A block diagram of the proposed 1720-MHz FM Transmitter.

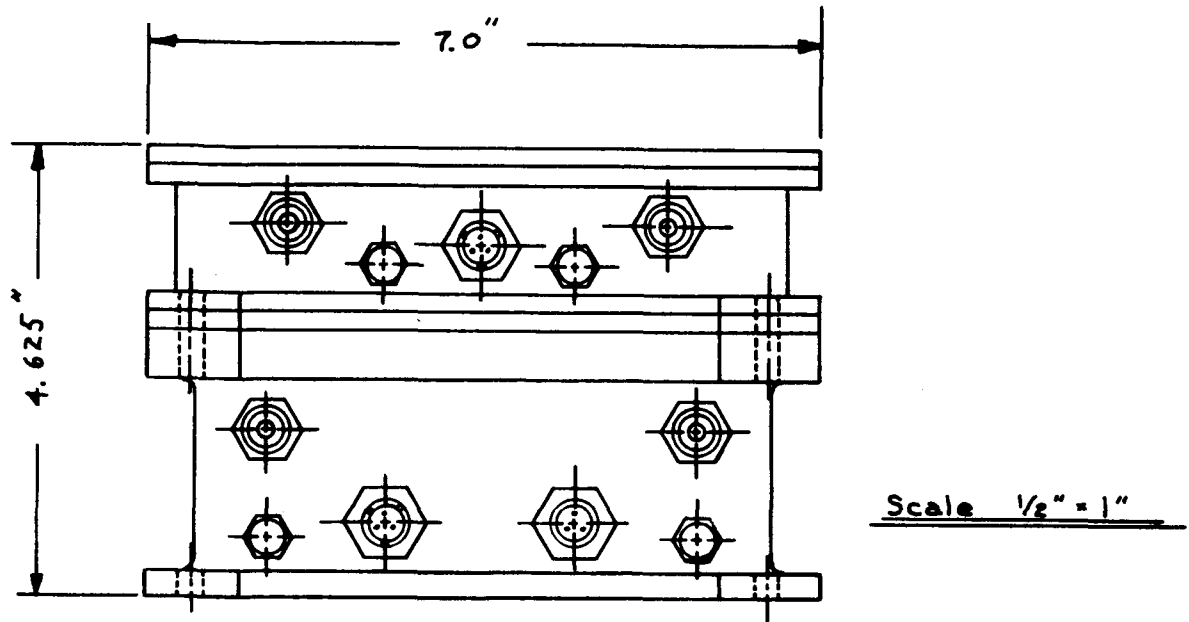


Fig. 2--End view of the proposed transmitter cases

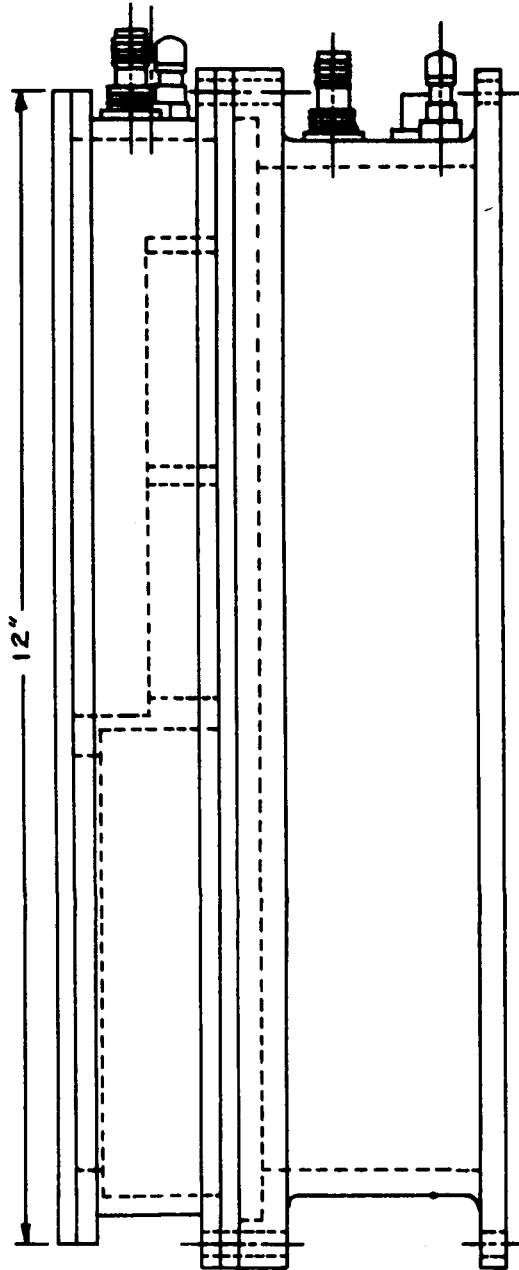


Fig. 3--Side view of the proposed transmitter cases.

circuit components for tuning and adjustment. The power amplifier case will provide a mount for two amplifiers and a power supply. Each case will be fabricated from a solid aluminum block.

#### 1. Exciter Unit

The exciter unit will consist of the exciter and an accompanying dc to dc converter. A block diagram of the exciter is presented in Figure 4. This section has seven major sub-sections: (1) the video amplifier and clamping circuits, (2) the voltage-controlled oscillator, (3) the transistor frequency multiplier, (4) the radio-frequency amplifier chain, (5) the diode frequency multiplier, (6) the automatic frequency control circuits, and (7) the circuitry to provide the keying pulse for the automatic frequency control loop. The block diagram for the proposed dc to dc converter, to be used with the exciter, is shown in Figure 5. The dc to dc converter also has seven major sub-sections, as shown in the diagram.

##### a. Video Amplifier and Clamping Circuit

The video amplifier section will accept an input signal (either polarity) of 1.4 volts peak-to-peak, and produce a clamped output waveform. This section will feature integrated-circuit amplifiers and a keyed clamping circuit. The video bandwidth will be 5 Hz to 10 MHz.

##### b. Voltage-Controlled Oscillator

The signal from the video amplifier will modulate a voltage-controlled Clapp oscillator by means of a varactor diode that is connected to the tank circuit of the oscillator. The oscillator will deviate from 106.875 MHz to 108.125 MHz corresponding to the maximum modulating signal swing. This

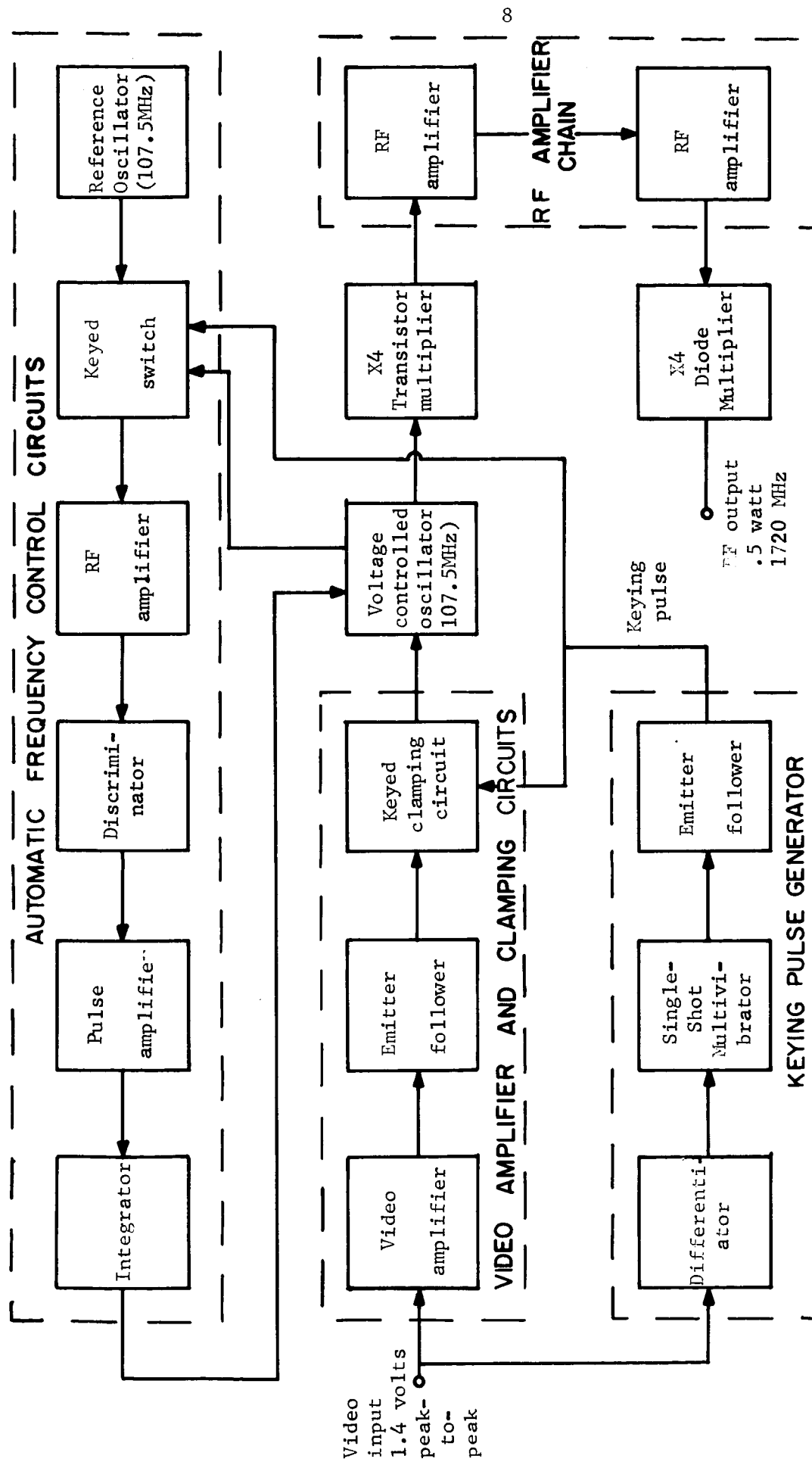


Fig. 4--A block diagram of the proposed 1720-MHz exciter.

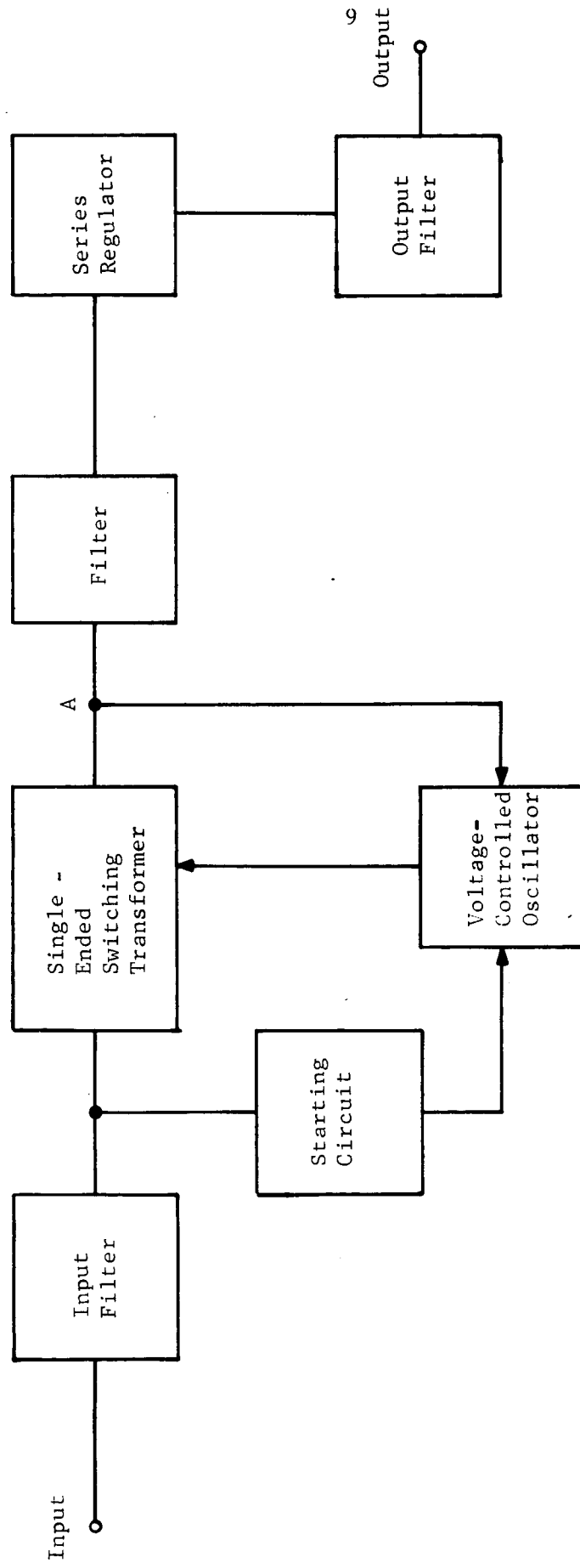


Fig. 5--A block diagram of the proposed dc to dc converter for the exciter.

variation will produce a peak-to-peak deviation from 1710 to 1730 MHz at the output of the exciter unit.

c. Transistor Frequency Multiplier

The transistor frequency multiplier will multiply the frequency-modulated RF signal from the oscillator by a factor of four. A common-emitter power amplifier operating in the class-C mode, which has an output that is rich in harmonics, will be used for this purpose. With state-of-the-art transistors, an approximate power of 100 mW is anticipated at the output of the multiplier.

d. Radio Frequency Amplifier Chain

The amplifier chain of the exciter unit will consist of two common-emitter power amplifiers in cascade. With the capabilities of available transistors, a gain of 15 db can be obtained with the two amplifiers in cascade. This will produce the output of two watts, which is required at the input of the diode multiplier in order to produce the exciter output of 0.5 watt.

e. Diode Frequency Multiplier

The diode multiplier will accept the output of the power amplifier chain, and will multiply this frequency by four. This multiplier will use a Motorola type MV18083 step-recovery diode.

f. Automatic Frequency Control Loop

The rest frequency of the voltage-controlled oscillator will be corrected by an automatic frequency control system designed to maintain the clamped oscillator frequency within .005 percent for a temperature range of  $-20^{\circ}\text{C}$  to  $+80^{\circ}\text{C}$ . The AFC loop will feature a keyed switch to provide a means of comparing a crystal reference oscillator signal with the

voltage-controlled oscillator signal. The switch will allow the voltage-controlled oscillator signal to be sampled only when there is no information modulating the VCO. The keyed switch will use PIN diodes to perform the switching function. The circuitry, which will provide the pulse to bias the appropriate PIN diode into the "on" condition, will be discussed in the succeeding section.

When the rest frequency signal from the VCO is sampled by the switch, it will be fed through an RF amplifier to a frequency discriminator. If the VCO signal is different in frequency from the reference oscillator signal, the discriminator will produce an output pulse proportional to the difference in frequency. The output pulse from the discriminator will be fed to a pulse amplifier and then to an integrating circuit. The integrator will produce a d-c bias voltage that is applied directly to the varactor diode in the tank circuit of the VCO. This adjusts the bias voltage on the varactor, which in turn changes the varactor capacitance, and adjusts the rest frequency of the voltage-controlled oscillator.

#### g. Keying Pulse Generation

The keying pulse, used for keying the d-c restoring circuit and the VCO frequency sampling, will be generated by stripping prominent periodic portions from the video input signal. The stripped portions will trigger a pulse generator, which will produce a pulse in synchronism with the video. The occurrence of the pulse is chosen to coincide with periods in the modulating signal, where there are no variations in the modulating signal. This value of signal establishes a reference for the d-c



component of the signal and a "rest" frequency for the oscillator.

In the case of a television input signal, the keying pulse occurs during the horizontal sync pulse of the television waveform.

#### h. Dc to Dc Converter

The power for the exciter unit will be supplied by a single-ended switching-transformer dc to dc converter. This converter will provide both a positive and a negative 28 volts dc output. The positive 28 vdc output will have a regulation of  $\pm 0.1$  percent and provide a maximum current of one ampere. The negative 28 vdc output will have a regulation of  $\pm 2.0$  percent and provide a maximum current of 100 milliamperes.

#### 2. Power Amplifier Unit

The proposed power amplifier unit consists of two planar triode cavity amplifiers operating at 1720 MHz, and an accompanying dc to dc converter to supply the necessary voltages. The amplifiers are expected to produce an over-all gain of 17 db providing an output power of 25 watts for a 0.5 watt input. An over-all bandwidth of 25 MHz is also expected.

The individual cavity amplifiers are expected to be similar in design and employ double, tuned-cavity output stages to provide the necessary bandwidth. The dc to dc converter will have a basic design similar to that planned for the exciter unit; but will provide high voltages on the order of 600 or 700 volts at 100 milliamperes for the plate circuits of the tubes, and filament voltages on the order of 6 volts at one ampere. The regulation for both outputs will be  $\pm 1.0$  percent.

### C. Exciter AFC Systems Analyses

Two AFC systems, which can provide the frequency stability of  $\pm .005$  percent desired for the exciter unit, were analyzed. Both systems employ gated, crystal-controlled, reference oscillators with stable output frequencies, which are compared to the VCO frequency. The stability of an exciter employing either system is largely determined by the reference oscillator stability. Both systems offer advantages and disadvantages which are to be discussed in the following sections.

#### 1. Discriminator AFC at an Intermediate Frequency.

##### a. System Analysis

The first system analyzed is shown in Figure 6. The output frequency of the VCO of 107 MHz is mixed with a crystal-controlled reference frequency of 97 MHz to provide an IF signal of 10 MHz. The reference-frequency oscillator output is gated by a gating pulse which occurs in synchronism with periodic portions of the modulating signal. (An example is the periodic sync tip of a television signal, during which the instantaneous frequency of the VCO ideally remains constant).

The IF signal is amplified in the IF amplifier, then presented to both the narrow-band and the wide-band discriminators. The wide-band discriminator allows a wide capture range of the VCO frequency prior to lock-in by the narrow-band (crystal) discriminator. The wide capture range is necessary since the frequency drift, as a result of the basic instability of the VCO, is greater than the bandwidth of the crystal discriminator.

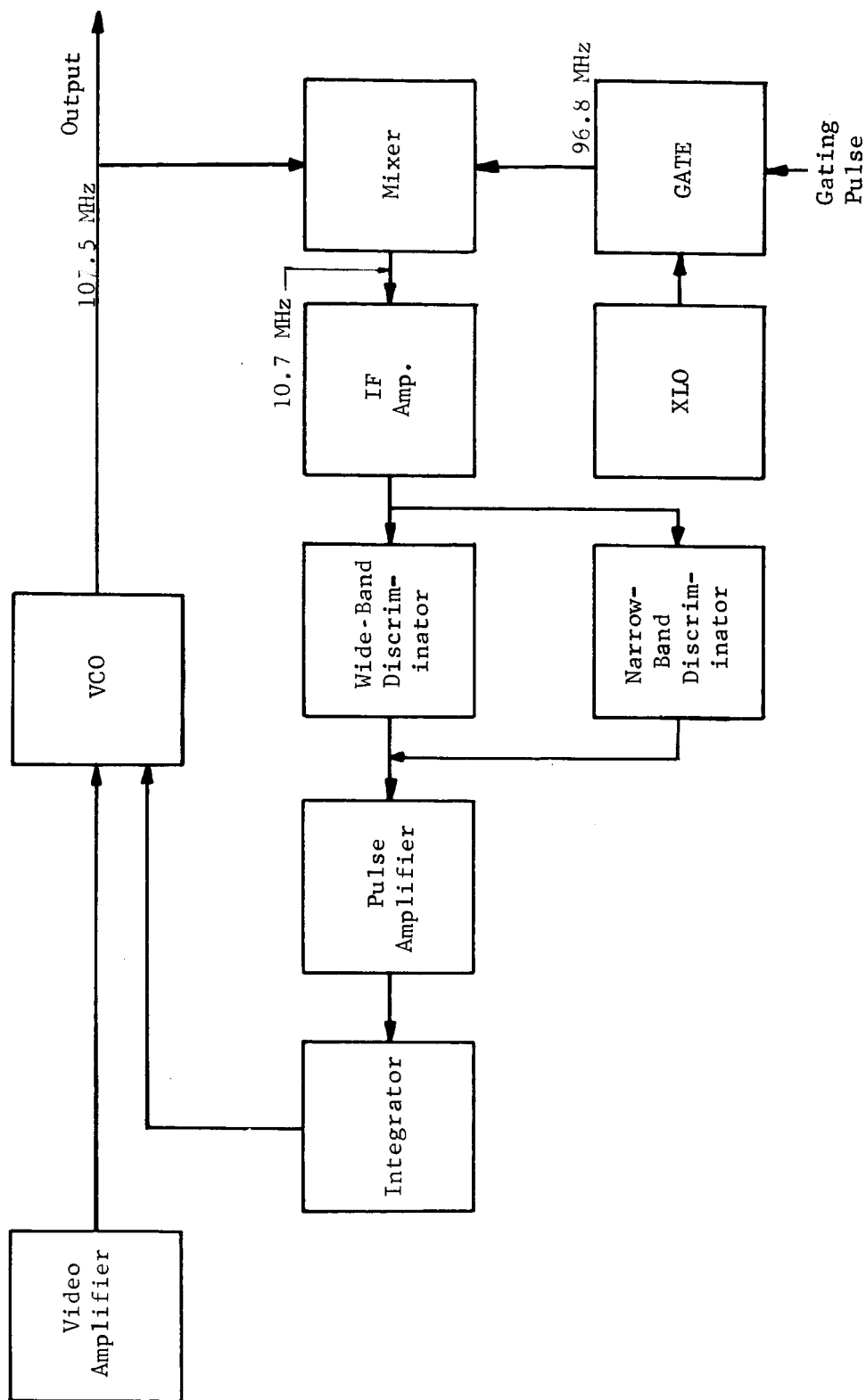


Fig. 6--Block diagram of an intermediate-frequency discriminator AFC system.

The output of the discriminators, which is a pulse of varying amplitude and polarity dependent upon the deviation of the IF frequency from the discriminator center frequency, is amplified in the pulse amplifier; then presented to the integrator. The integrator consists mainly of a low-pass filter with a cutoff frequency substantially below the AFC pulse repetition frequency.

The output of the integrator is a slowly varying d-c signal proportional to the frequency drift of the VCO. It is summed with the video modulating signal in the VCO modulating circuit to provide the necessary frequency correction.

The intermediate-frequency AFC system is shown in block diagram form in Figure 6. It can be reduced to that of Figure 7, where the symbols are defined in the s-domain as follows:

- $V_m$  - the modulating signal voltage,
- $K_1$  - the VCO modulation constant expressed in Hz/volt,
- $K_2$  - the narrow-band discriminator conversion constant expressed in volts/Hz,
- $K_3$  - the wide-band discriminator constant expressed in volts/Hz,
- $K_4$  - the open-loop gain due to the amplifiers, the mixer, the integrator, coupling factors, etc.,
- $G(s)$  - the frequency-dependent factor of the open-loop transfer function; largely the low-pass filter transfer function,
- $F_o$  - the output frequency,
- $F_m$  - the instantaneous component of  $F_o$  due to modulation and compensation,
- $F_v$  - the uncorrected frequency of the VCO,

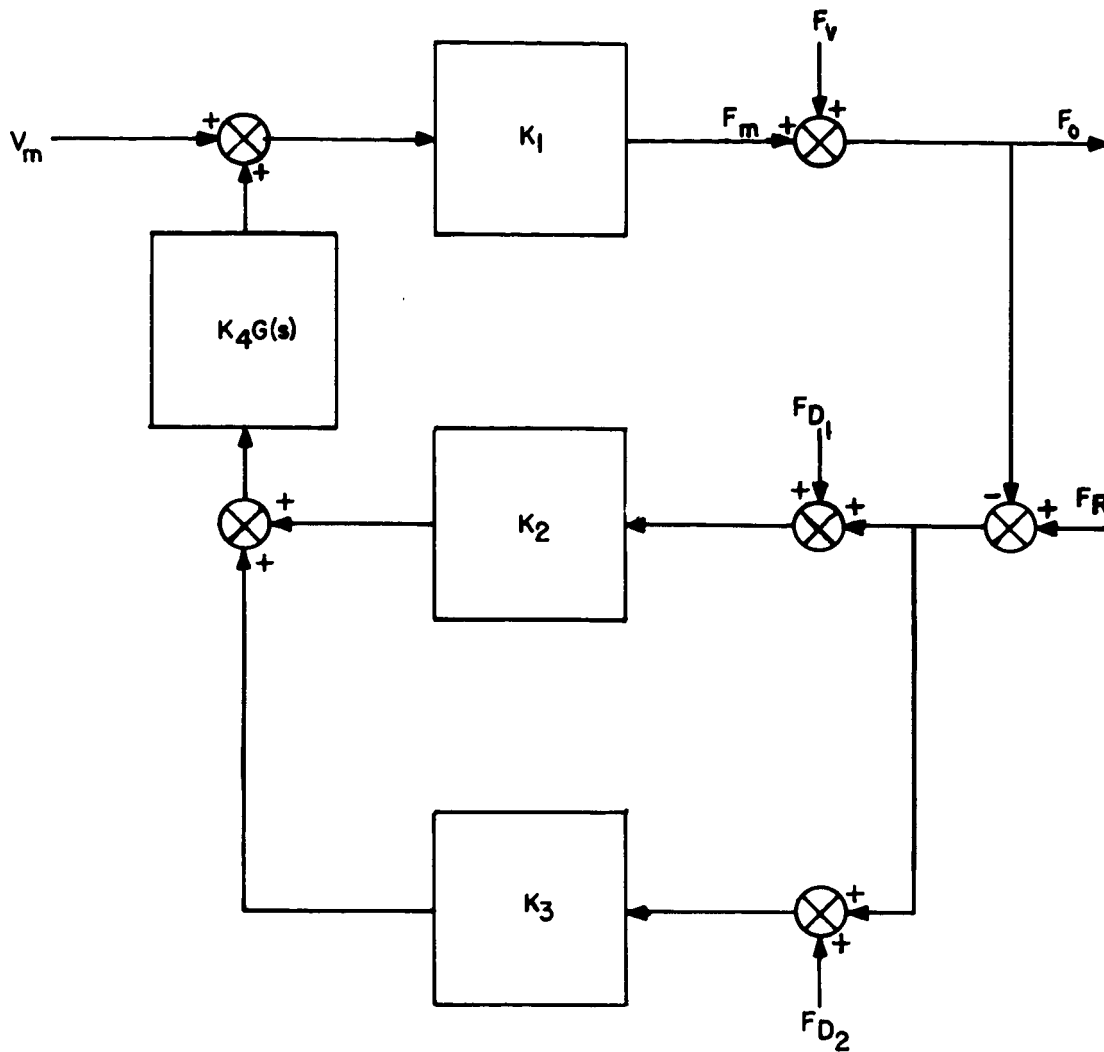


Fig. 7--Simplified block diagram of an intermediate-frequency discriminator AFC system.

$F_R$  - the reference frequency,

$F_{D1}$  - the center frequency of the narrow-band discriminator,

and

$F_{D2}$  - the center frequency of the wide-band discriminator.

By block diagram algebra the diagram of Figure 7 can be further reduced to that shown in Figure 8 where  $K = K_1 (K_2 + K_3) K_4$ , and the modulation voltage is ignored. The latter is possible since the gated AFC system compares the VCO frequency during a period of constant level of the modulating signal. Thus, the desired output frequency of the VCO is a constant during the sampling periods. As shown in Figure 8,

$$F_O = F_V + F_m \quad (1)$$

and

$$F_m = K G(s) [F_D + (F_R - F_O)], \quad (2)$$

where

$$F_D = \frac{K_2}{K_2 + K_3} F_{D1} + \frac{K_3}{K_2 + K_3} F_{D2} . \quad (3)$$

If equation (1) and (2) are combined,

$$F_O = F_V + K G(s) (F_D + F_R) - K G(s) F_O$$

or

$$F_O = \frac{F_V + K G(s) (F_D + F_R)}{1 + K G(s)} . \quad (4)$$

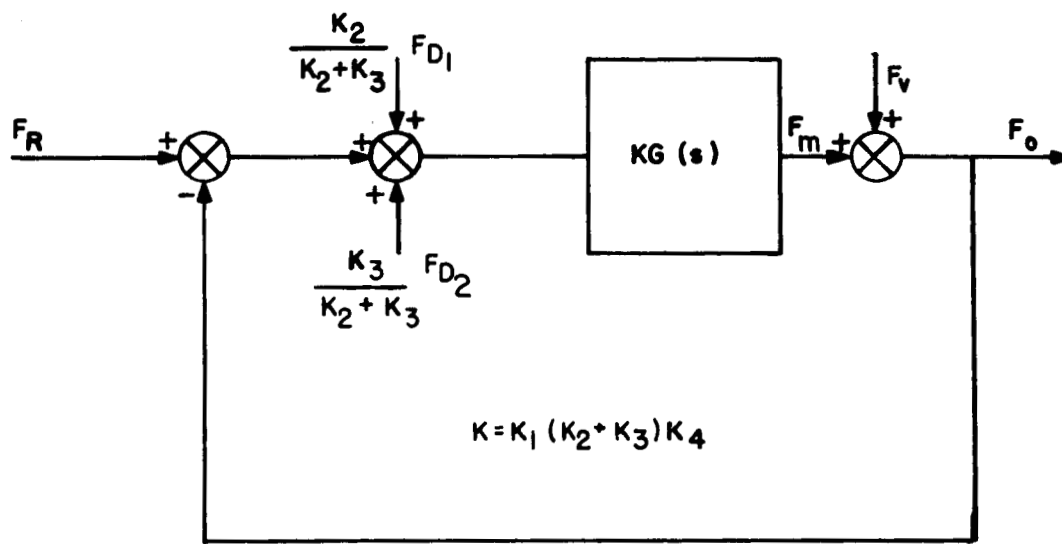


Fig. 8--Further simplified block diagram of an intermediate-frequency discriminator AFC system.

If a single-section, low-pass, RC filter is used, then,

$$G(s) = \frac{1/RC}{s + 1/RC} \quad (5)$$

Upon substitution of equation (5) into equation (4),

$$F_o = \frac{F_v}{1 + K \frac{1/RC}{s + 1/RC}} + K \frac{1/RC}{s + 1/RC} \cdot \frac{F_D + F_R}{1 + K \frac{1/RC}{s + 1/RC}} \quad (6)$$

If  $F_v$ ,  $F_D$ , and  $F_R$  are considered as constants, then by the final value theorem,

$$\lim_{t \rightarrow \infty} f(t) = \lim_{s \rightarrow 0} s F(s), \quad (7)$$

the output frequency is obtained

$$f_o = \frac{f_v}{1 + K} + K \frac{f_D + f_R}{1 + K} \quad (8)$$

Upon rearrangement,

$$f_o = f_R + f_D + \frac{f_v - (f_R + f_D)}{1 + K}, \quad (9)$$

indicating that the output frequency is the sum of the reference oscillator frequency, the composite discriminator center frequency, and an error term which is inversely proportional to the open-loop gain  $K$ .



The effects on the frequency of the various component stabilities may be determined by using a variation of equation (8). Let primed variables denote design center values, then

$$f'_o + \delta_o f'_o = \frac{f'_v + \delta_v f'_v}{1 + K} + \frac{K}{1 + K} (f'_R + \delta_R f'_R + f'_D + \delta_D f'_D) . \quad (10)$$

Since the primed variables denote design center values, where

$$f'_o = f'_v = f'_R + f'_D , \quad (11)$$

the expression (10) is reduced to

$$\delta_o f'_o = \frac{\delta_v f'_v}{1 + K} + \frac{K}{1 + K} (\delta_R f'_R + \delta_D f'_D) \quad (12)$$

by subtracting out  $f'_o$  from both sides of equation (10). The  $\delta$  terms are stability factors for the frequency determining elements of the AFC loop. The factors are dimensionless and may be positive or negative and are expressed in percent or parts per million parts.

From equation (12), it is seen that for large values of gain ( $K \gg 1$ ),

$$\delta_o f'_o = \frac{\delta_v f'_v}{K} + \delta_R f'_R + \delta_D f'_D . \quad (13)$$

Therefore, the frequency error in Hertz is the algebraic sum of the following: (1) the amount the reference oscillator is off the design

center frequency, (2) the amount the composite discriminator is off its design center frequency, and (3) an amount proportional to the basic instability of the VCO and inversely proportional to the open-loop gain of the system.

An expression of the output frequency stability is obtained from equation (13) by factoring out  $f'_o$  from both sides. Thus,

$$\delta_o = \frac{\delta_v}{K} + \frac{f'_R}{f'_o} \delta_R + \frac{f'_D}{f'_o} \delta_D . \quad (14)$$

The polarity of the frequency drift or instability is determined from the polarities of the individual instabilities and their relative magnitudes. However, on investigation of equation (14), it is seen that the maximum instability occurs when all terms have the same polarity. The properly designed system corrects for this event and, on that basis, the required value of gain K for a desired output stability can be calculated. The gain factor K is solved for in equation (14),

$$K = \frac{\delta_v}{(\delta_o - \delta_R) - (\delta_D - \delta_R) \frac{f'_D}{f'_o}} . \quad (15)$$

Curves illustrating equations (14) and (15) are shown in Figures 9 and 10 respectively, where typical values of  $\delta_v$ ,  $\delta_D$ ,  $\delta_R$ , and the ratio of  $f'_D/f'_o$  are assumed.

#### b. Composite Discriminator

A discussion of the composite discriminator formed by the parallel arrangement of narrow-band and wide-band discriminators is worthwhile.

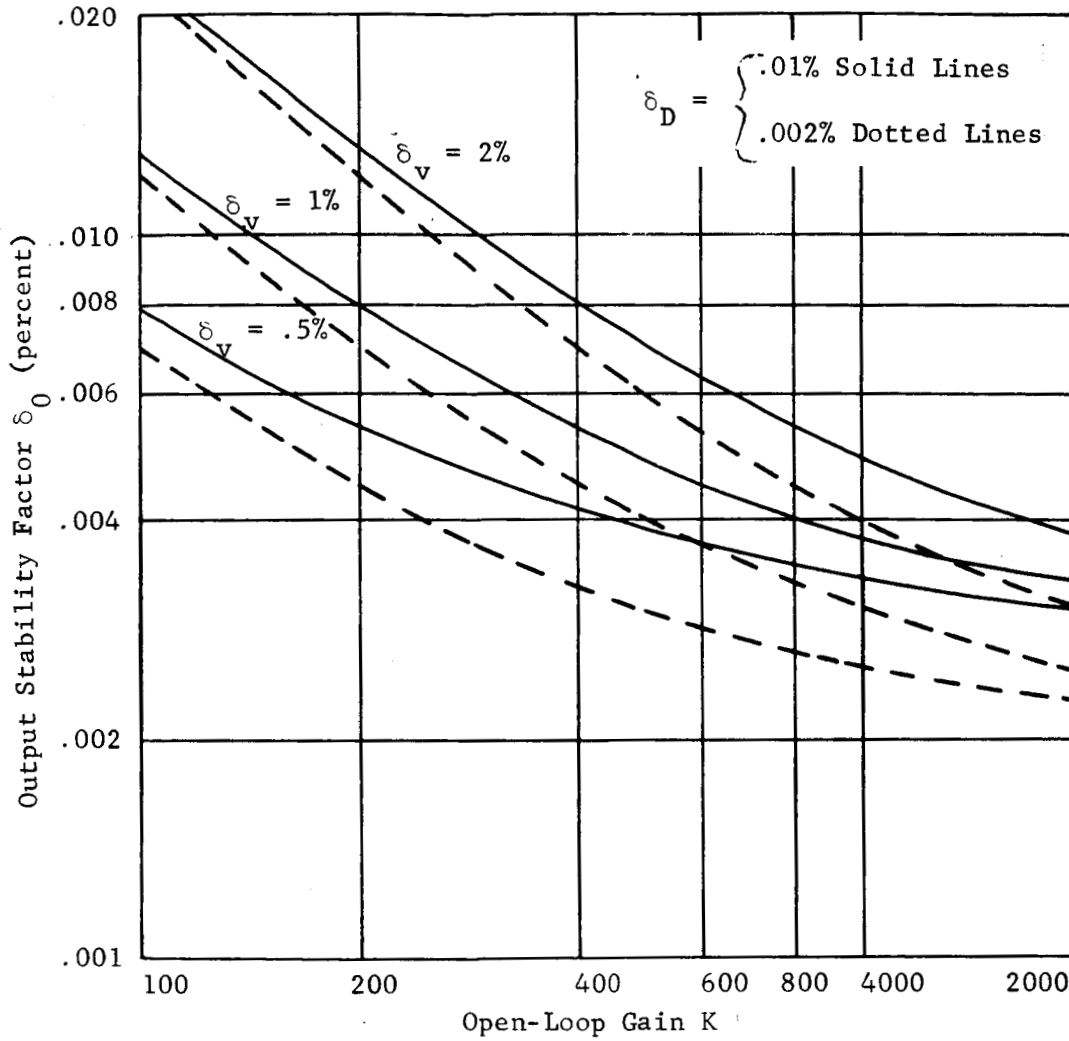


Fig. 9--Curves showing the output frequency stability factor as a function of open-loop gain  $K$ , VCO stability factor  $\delta_v$ , and discriminator stability factor  $\delta_D$ . The reference oscillator stability factor  $\delta_R$  is assumed to be .002 percent and  $f'_D/f'_O = 0.1$ .

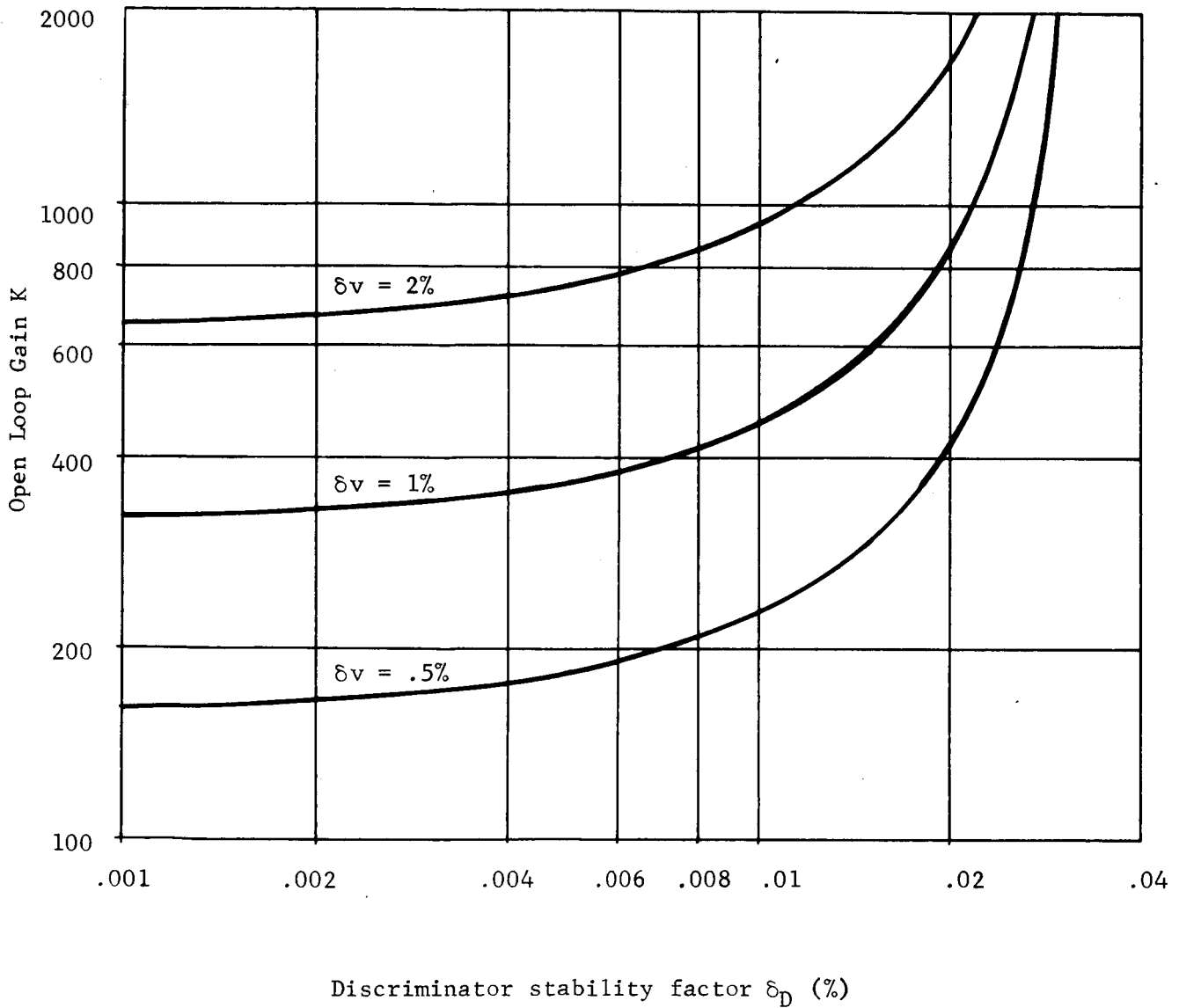


Fig. 10--Curves showing the required open-loop gain K for a required output stability factor of .005 percent as a function of the discriminator stability factor  $\delta_D$  and the VCO stability factor  $\delta_v$ . The reference oscillator stability factor  $\delta_R$  is assumed to be .002 percent and  $f'_D/f'_O = 0.1$ .

According to Figure 11, the parallel discriminators of (a) reduce to the composite of (b), where

$$F_D = \frac{K_2}{K_2 + K_3} F_{D1} + \frac{K_3}{K_2 + K_3} F_{D2}, \quad (16)$$

and

$$K = K_2 + K_3.$$

The frequency drift contributed by the instabilities of the two discriminators is given by

$$\delta_D f'_D = \delta_{D1} \frac{K_2}{K_2 + K_3} f'_{D1} + \delta_{D2} \frac{K_3}{K_2 + K_3} f'_{D2}. \quad (17)$$

Since  $f'_D = f'_{D1} = f'_{D2}$ ,

$$\delta_D = C_1 \delta_{D1} + C_2 \delta_{D2} \quad (18)$$

where  $C_1$  and  $C_2$  are the weighting constants,

$$C_1 = \frac{K_2}{K_2 + K_3} \quad \text{and} \quad C_2 = \frac{K_3}{K_2 + K_3}. \quad (19)$$

A possible difficulty in the use of parallel discriminators is the requirement of a relatively low stability factor for the wide-band discriminator. The composite discriminator curve will contain more than

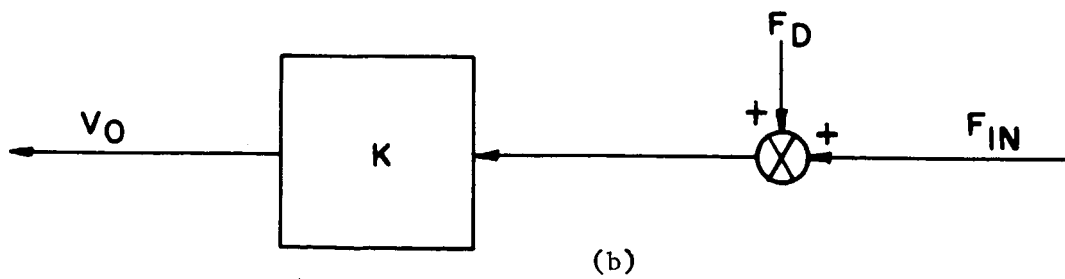
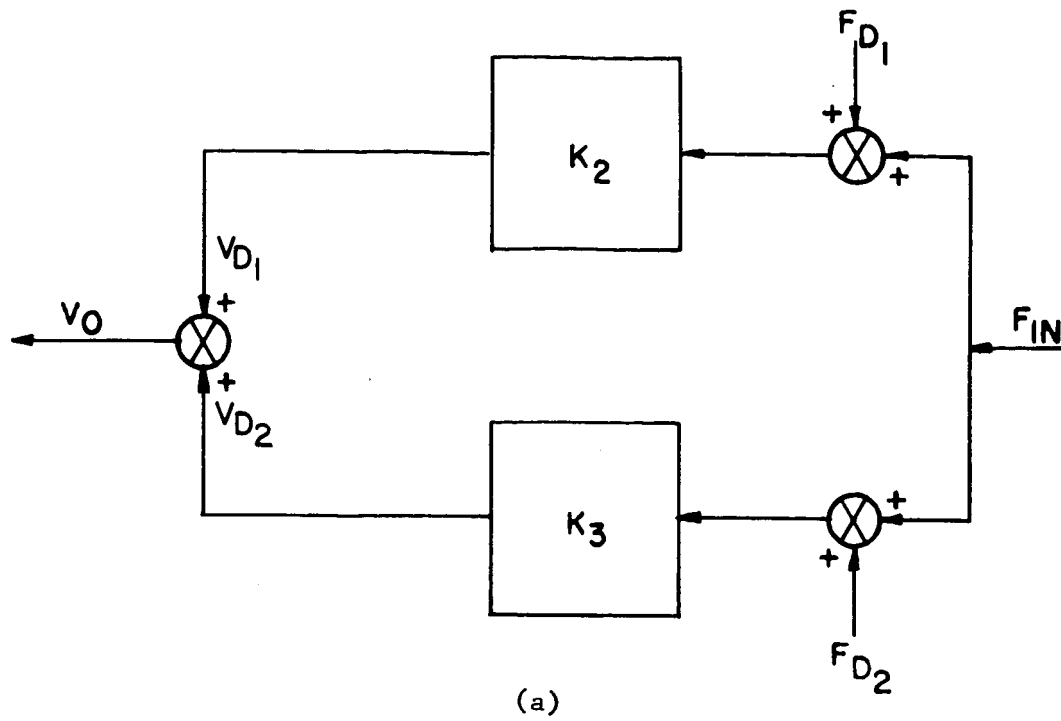


Fig. 11-Block diagrams of the parallel discriminator (a) and the composite discriminator (b).

one zero-crossing if the instability of the center frequency of the wide-band discriminator is greater than one-half the bandwidth of the narrow-band discriminator. This is illustrated in Figure 12 for idealized discriminator curves. In addition, to provide for the possibility of having stability factors of opposite polarity for the two discriminators, the allowed instability of the wide-band discriminator must be further reduced by the stability factor of the narrow-band discriminator. In equation form, the allowed instability of the wide-band discriminator is

$$|\delta_{D_2}| f'_D \leq \left[ \frac{BW_{D_1}}{2} - |\delta_{D_1}| f'_D \right] \quad (20)$$

Consider the following typical case of a crystal discriminator and a wide-band discriminator operating at 10 MHz with a wide-band bandwidth of 2 MHz. Typical values for the crystal discriminator are: stability factor,  $\delta_{D_1} = \pm .005\%$  and bandwidth,  $BW_{D_1} = .2\%$ . From equation 20,

$$|\delta_{D_2}| f'_D \leq \left[ \frac{.2\% f'_D}{2} - .005\% f'_D \right]$$

or

$$|\delta_{D_2}| \leq .095\%$$

A stability factor of .095% requires careful selection of components and, possibly, certain methods of compensation for temperature induced frequency drift. For example, if the discriminators are operated over

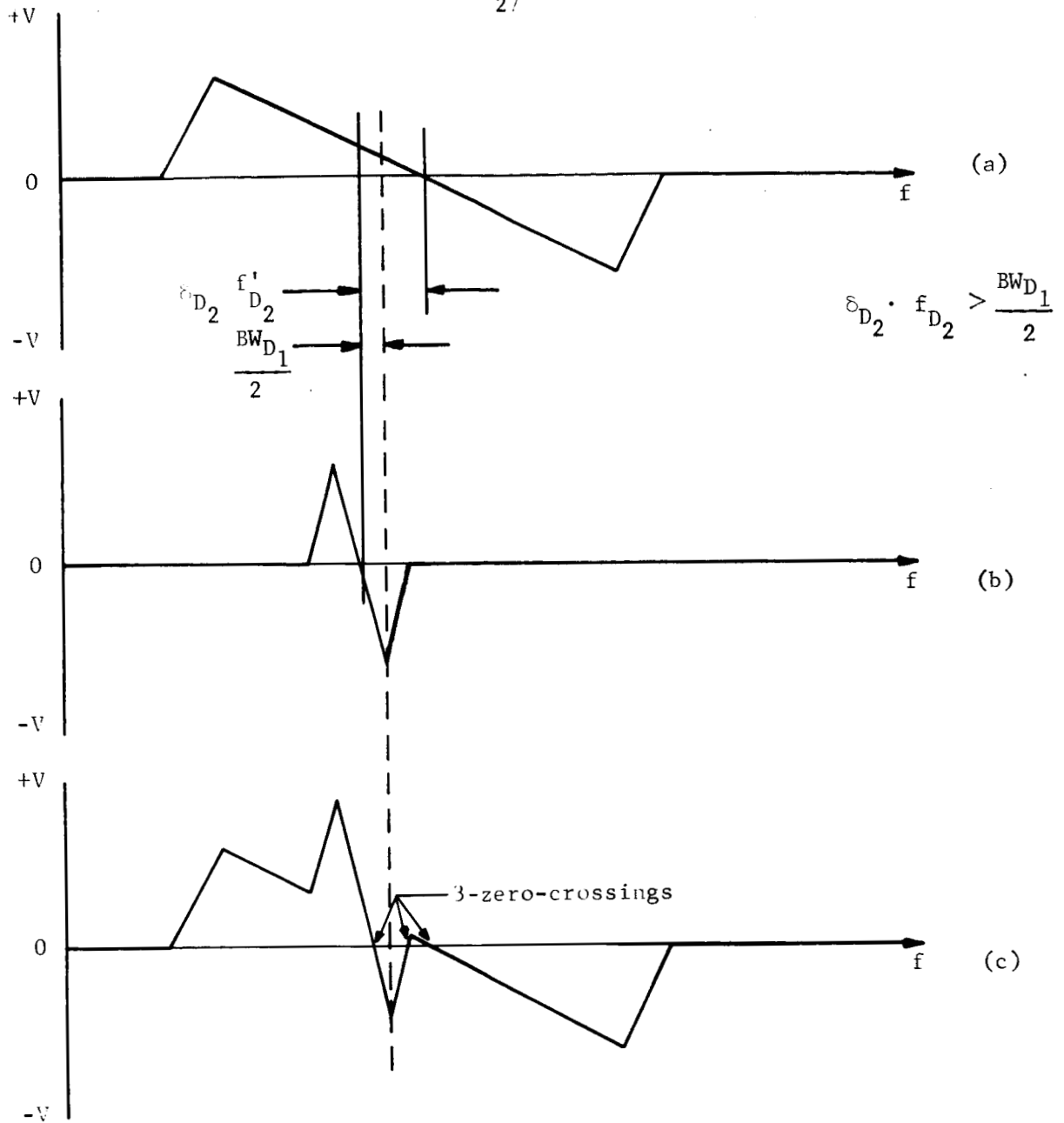


Fig. 12--Idealized discriminator curves for a wide-band (a) and a narrow-band (b) discriminator and a composite curve (c) for the two in parallel. The composite curve has three zero-crossings due to a center frequency drift of the wide-band discriminator that is greater than one-half the bandwidth of the narrow-band discriminator.



a temperature range of  $100^{\circ}$  Celsius, the stability factor of .095% represents a stability of 9.5 ppm/ $^{\circ}$ C for the over-all circuit. This factor is less than that usually quoted by some manufacturers for "zero" temperature coefficient components.

The gain factors,  $K_2$  and  $K_3$ , for the discriminators are given by

$$K_2 = \frac{V_p}{BW_{D1}} \quad \text{and} \quad K_3 = \frac{V_p}{BW_{D2}} \quad (21)$$

where equal peak IF voltage  $V_p$  is assumed for both discriminators. For the typical case and values given,

$$K_2 = \frac{1}{.002} \frac{V_p}{f'_D} \quad \text{and} \quad K_3 = \frac{1}{.2} \frac{V_p}{f'_D} .$$

From equation (19),

$$C_1 = \frac{K_2}{K_2 + K_3} = \frac{1/.002}{1/.002 + 1/.20} = \frac{500}{505} = .99$$

and

$$C_2 = \frac{K_3}{K_2 + K_3} = \frac{1/.20}{1/.002 + 1/.20} = \frac{5}{505} = .01 .$$

The composite stability factor given by equation (18) is

$$\delta_D = C_1 \delta_{D1} + C_2 \delta_{D2}$$

or

$$\delta_D = .99 \delta_{D_1} + .01 \delta_{D_2} .$$

For the typical stability factors given for the discriminators,

$$\delta_D = .00293\% .$$

For this case, the stability factor for the composite discriminator greater than 33 over that of the wide-band discriminator. A further improvement can be obtained by inserting an additional gain factor in the narrow-band discriminator circuit to make the ratio  $C_1/C_2$  greater.

## 2. Gated Discriminator AFC at the Output Frequency.

The second AFC system analyzed is shown in Figure 13. The output frequency of the voltage-controlled oscillator at approximately 107 MHz is compared with the crystal-controlled reference frequency at 107 MHz. The two frequencies are alternately fed to the discriminator which provides an output of pulses whose amplitudes are proportional to the difference between the two frequencies. The discriminator is ac coupled to the detector, thus, removing the major effect that the discriminator center frequency stability has on the over-all stability of the system. (A second-order error, attributable to unequal input signals from the VCO and the reference oscillator, is caused by discriminator drift). The output from the discriminator is fed to a synchronous detector and low-pass filter whose output is subsequently applied to the VCO to affect necessary frequency-correction.

The AFC system shown in Figure 13 can be reduced to the diagram shown in Figure 14 where the parameters in the s-domain are:

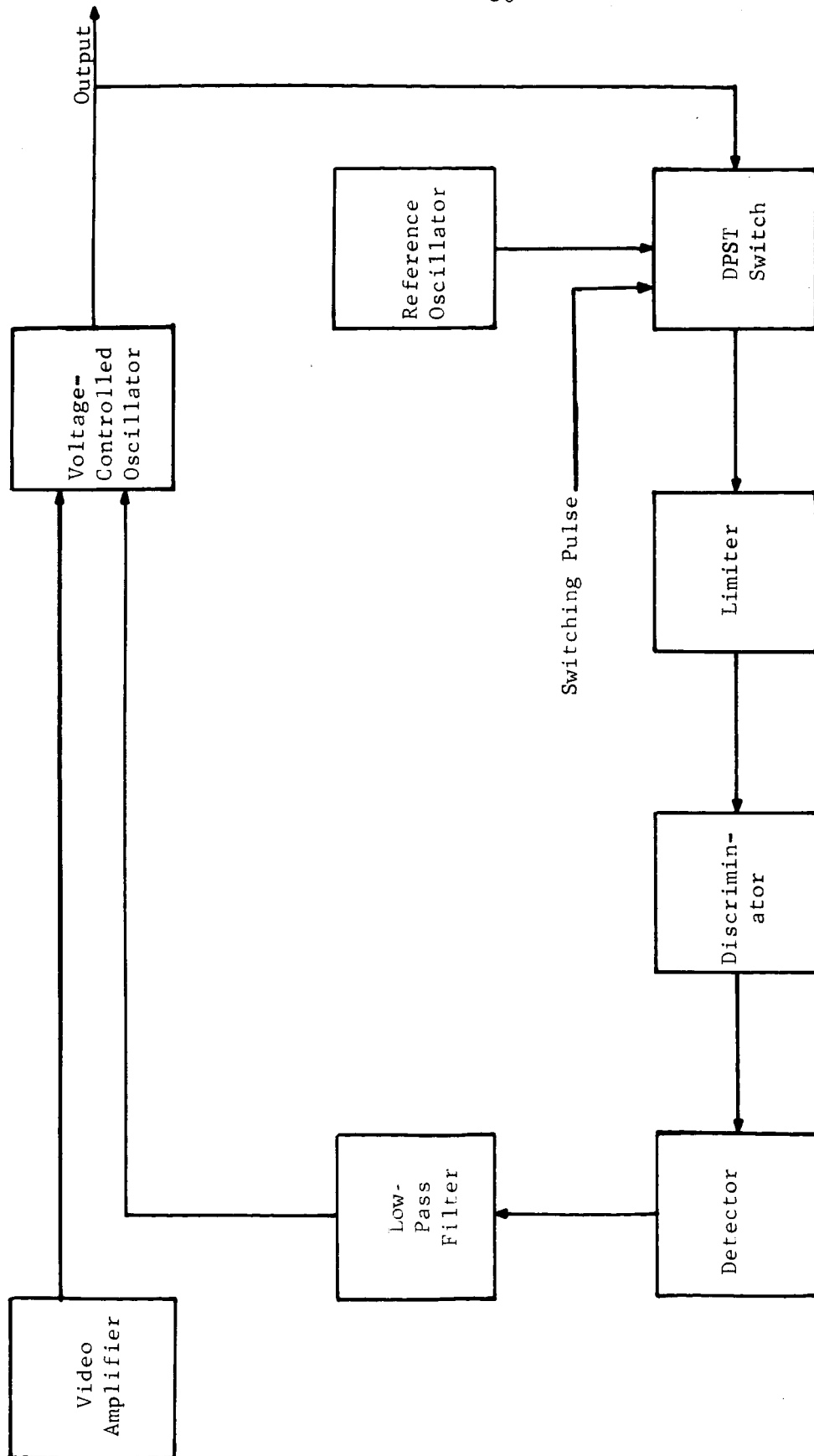


Fig. 13--Block diagram of a gated discriminator AFC system operating at the VCO frequency.

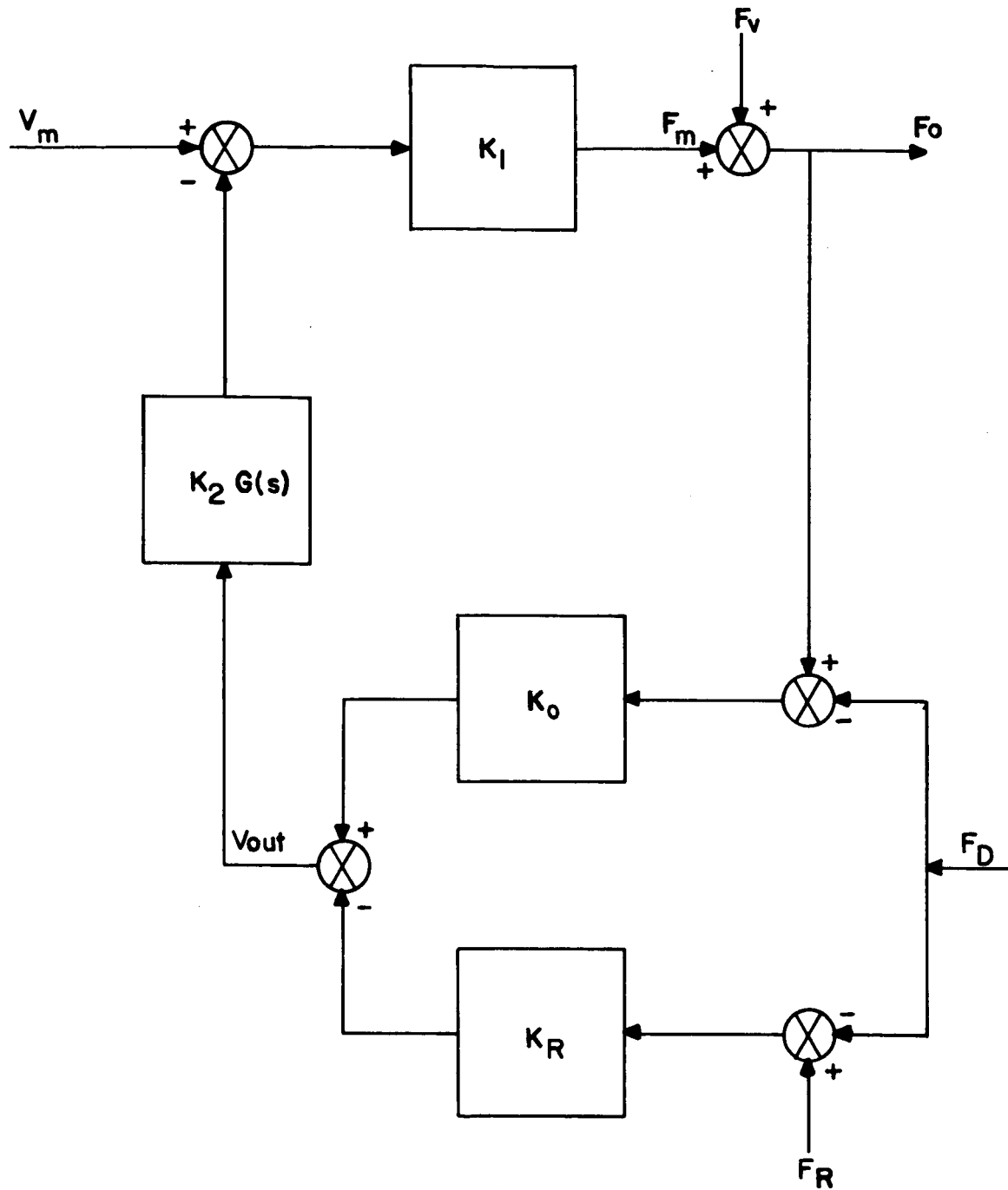


Fig. 14--Simplified block diagram of a gated discriminator AFC system operating at the VCO frequency.

$V_m$  - the modulating signal voltage,

$K_1$  - the VCO modulation constant expressed in Hertz/volt,

$K_2$  - the open-loop gain due to amplifier, the filter, the coupling factors, etc.,

$K_o$  - the discriminator conversion constant due to the VCO signal expressed in volts/Hertz,

$K_R$  - the discriminator conversion constant due to the reference signal expressed in volts/Hertz,

$F_M$  - the instantaneous component of  $F_o$  due to modulation and compensation,

$F_v$  - the uncorrected frequency of the VCO,

$F_o$  - the output frequency,

$F_R$  - the reference frequency,

$F_D$  - the center frequency of the discriminator,

$V_{out}$  - the discriminator output voltage,

and

$G(s)$  - the frequency-dependent factor of the open-loop transfer function.

According to Figure 14,

$$V_{out} = K_o(F_o - F_D) - K_R(F_R - F_D) \quad (1)$$

and

$$F_o = F_v - K_1 K_2 G(s) V_{out} + K_1 V_m \quad (2)$$

If the VCO output frequency is sampled periodically during periods when the video input is not varying and the level of video is the same during each sample, the output frequency attributable to the modulation is zero. This would be the case if the video signal were a television signal and the sampling done during the horizontal sync-pulse interval. If equations (1) and (2) are combined

$$F_o = \frac{F_v + K(s) K_o F_D + K(s) K_R (F_R - F_D)}{1 + K(s) K_o} \quad (3)$$

where  $K(s) = K_1 K_2 G(s)$ . Let the frequency-dependent factor of the transfer function be determined by a single-section low-pass filter, then,

$$G(s) = \frac{1/RC}{s + 1/RC} \quad (4)$$

By the final value theorem,

$$f_o = \frac{1}{1 + K_1 K_2 K_o} f_v + \frac{K_1 K_2 K_o}{1 + K_1 K_2 K_o} f_D + \frac{K_1 K_2 K_R}{1 + K_1 K_2 K_o} (f_R - f_D) \quad (5)$$

If  $K_1 K_2 K_o \gg 1$ , as is generally the case, then

$$f_o = \frac{1}{K_1 K_2 K_o} f_v + \frac{K_R}{K_o} f_R + \left(1 - \frac{K_R}{K_o}\right) f_D \quad (6)$$

The system stability factor can be determined from equation (6) by letting,

$$\begin{aligned}
f_o &= f_o' + \delta_o f_o' \\
f_v &= f_v' + \delta_v f_v' \\
f_R &= f_R' + \delta_R f_R' \\
f_D &= f_D' + \delta_D f_D'
\end{aligned}
\tag{7}$$

where the primed values are design values and the  $\delta$  factors are stability factors expressed in percent. After the substitutions from (7) into equation (6)

$$\begin{aligned}
f_o' + \delta_o f_o' &= \frac{1}{K_1 K_2 K_o} (f_v' + \delta_v f_v') + \frac{K_R}{K_o} (f_R' + \delta_R f_R') \\
&+ \left(1 - \frac{K_R}{K_o}\right) (f_D' + \delta_D f_D')
\end{aligned}
\tag{8}$$

Since the design values are the same,  $f_o' = f_v' = f_R' = f_D'$ , equation (8) reduces to

$$\delta_o = \frac{1}{K} \delta_v + \frac{K_R}{K_o} \delta_R + \left(1 - \frac{K_R}{K_o}\right) \delta_D
\tag{9}$$

where  $K = K_1 K_2 K_o$ .

Investigation of equation (9) shows, that for  $K_R = K_o$  and  $K$  very large, the output stability factor approaches that of the reference oscillator. The ratio  $K_R/K_o$  is determined by the ratio of the reference voltage to the output voltage that is fed to the discriminator. Good limiting is required prior to discrimination to insure that  $K_R$  is approximately equal to  $K_o$ .

The curves of Figure 15 illustrate equation (9) for the expected range of values for  $\delta_v$ ,  $\delta_R$ ,  $\delta_D$ ,  $K_R/K_O$ , and  $K$ . Typical values are:

$$\delta_v - \pm .5\% \text{ to } \pm 2\%$$

$$\delta_R - \pm .002\%$$

$$\delta_D - \pm .5\%$$

$$K_R/K_O - .995\% \text{ to } 1.005\%$$

$$K - 100 \text{ to } 2000.$$

The maximum instability occurs when all the component instabilities have the same sign. This condition is illustrated in Figure 15.

#### D. Peltier Temperature Chamber

Design and construction has been initiated on a Peltier thermoelectric environmental chamber. The Peltier system is designed to operate over a temperature range of  $-20^{\circ}\text{C}$  to  $+80^{\circ}\text{C}$ . The purpose of constructing the chamber is two-fold: (1) to study the feasibility of controlling the environment of a solid-state transmitter riding on board a space vehicle and (2) to have available a convenient environmental chamber to temperature test the electronic modules which combine to form a transmitter.

Design of the Peltier system involves three steps: (1) the selection of the thermoelectric unit to perform the desired environmental task, (2) the design of the actual chamber and the associated support system, and (3) the selection of the power supply.

A block diagram of the complete system is shown in Figure 16. The switch provides a means of reversing the system from the heating to the cooling mode or vice-versa. The chamber control panel provides a means



$$K_R/K_O = \begin{cases} .995; & \text{---} \\ .999; & \text{---} \\ 1.00; & \text{---} \end{cases}$$

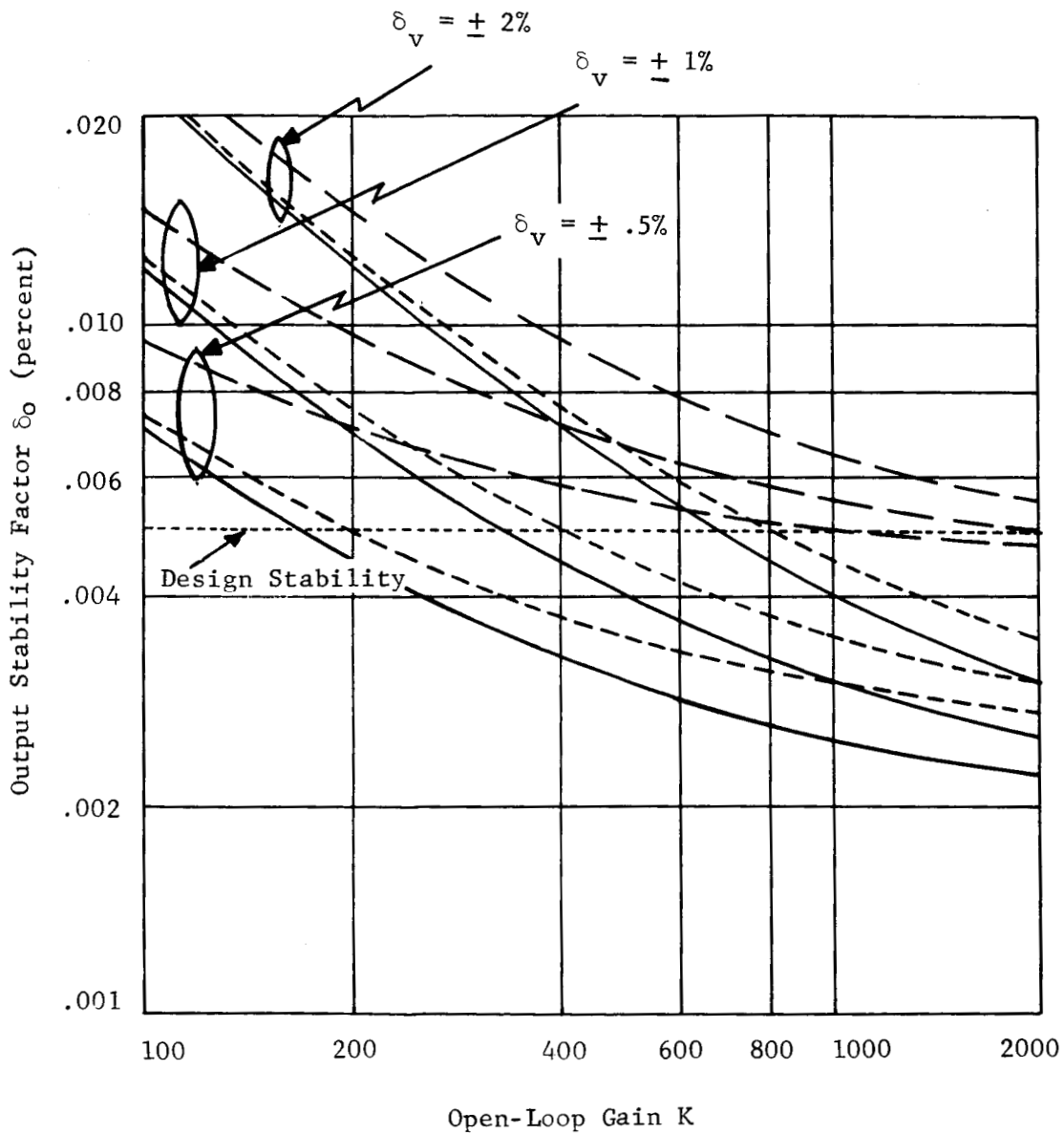


Fig. 15--Curves of the output stability factor  $\delta_O$  as a function of the open-loop gain  $K$ , the VCO stability factor  $\delta_V$ , and the ratio  $K_R/K_O$ . The reference stability factor  $\delta_R$  and discriminator stability factor  $\delta_D$  are assumed constant at  $\pm 0.002$  percent and  $\pm 0.5$  percent, respectively.

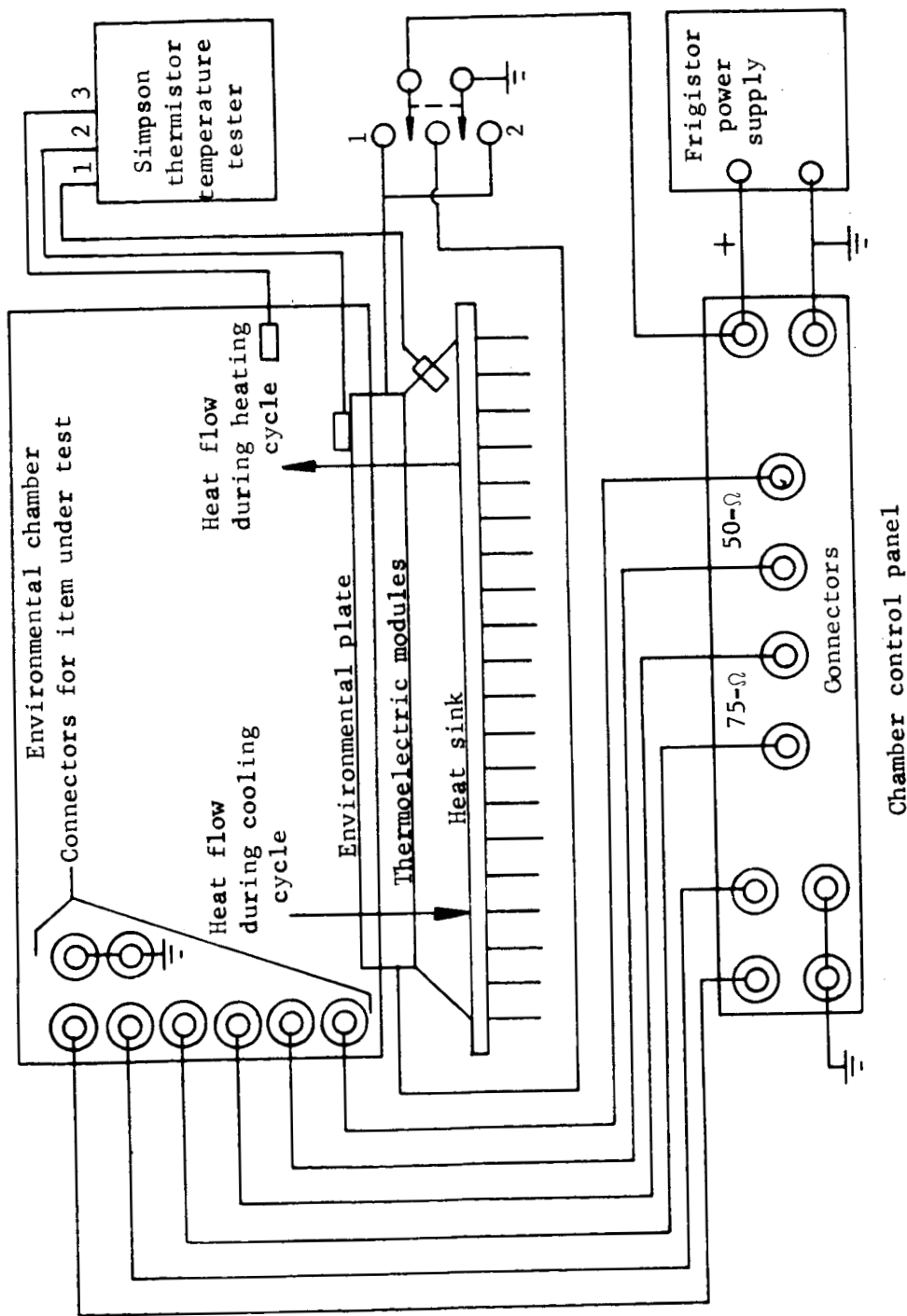


Fig. 16.-A block diagram of the Peltier thermoelectric environmental chamber.

to monitor the operation of the item under test. On the control panel there are provided two coaxial cable connectors with 50-ohm cable leading into the chamber enclosure, two coaxial cable connectors with 75-ohm cable leading into the enclosure and two sets of binding posts, intended primarily for dc use. Power for driving the thermoelectric modules is provided by the Frigistor power supply, a 30-ampere supply purchased from Frigistors, Limited. The Simpson thermistor temperature tester provides a means by which three different temperatures may be monitored simultaneously. The temperatures monitored are the heat sink, the environmental plate and the item under test.

Tests are currently underway which will result in data and curves describing the operation of the Peltier system. The data gathered will provide a criterion for further discussing the advantages and limitations of the system.

## II. MILLIMETER WAVES STUDY

During the summer a study of attenuation in oversized circular waveguide was conducted. The study consisted of an experiment on a 60-foot section and a measurement of the attenuation versus the waveguide-straightness. The results indicated that the 100-foot section of circular waveguide used for the environmental chamber need not be unreasonably straight to obtain low attenuation. In addition, the results indicated that the attenuation increased approximately one db per gigacycle when the frequency deviated from the center frequency of the rectangular to circular waveguide coupler. This indicated that the center frequency of these waveguide transitions played an important part in determining the transmitted frequency used in each band.

Construction of the environmental chamber components was continued, and the Fresnel-Zone Lenses are being made.